Energy & Environmental Science

ARTICLE

Highly Selective CO Removal by Sorption Enhanced Boudouard Reaction for Hydrogen Production

Received 00th January 20xx,
Accepted 00th January 20xx

DOI: 10.1039/x0xx00000x

www.rsc.org/

Kumar R Rout[a]*, María V Gil[b] and De Chen[b]*

Development of an energy-efficient and cost-effective technology for purification of a hydrogen rich stream to achieve CO concentration below 10 ppm, suitable for low temperature fuel cell applications, is one of major objectives of energy research. Here we report the sorption enhanced Boudouard (SEB) reaction as an effective route for pure hydrogen production on metal-free catalysts by highly selective removal of CO and CO_2 from a hydrogen rich stream, where CaO serves as both catalyst and CO_2 sorbent. We reveal that the in-situ generated oxygen vacancy by CO adsorption on CaO catalyzes the sorption enhanced Boudouard reaction, hence Boudouard reaction and CO_2 removal occurring simultaneously in a single step. The capture of CO_2 in the presence of H_2 by the solid sorbent shifts the chemical equilibrium towards the complete CO conversion. The results demonstrate a remarkable decrease in the CO concentration from 0.5% in a hydrogen rich stream to less than 5 ppm, suitable for low temperature fuel cells. It avoids a subsequent preferential oxidation process or methanation reaction, as well as an additional CO_2 capture process. The feasibility of applying the sorption enhanced Boudouard reaction in the production of highly pure hydrogen (CO content less than 10 ppm) was demonstrated by multicycle tests of Boudouard-carbonation/regeneration on Ca-based oxides with stable cyclic operation.

1. Introduction

It is widely accepted that hydrogen is an environmentally friendly and clean energy carrier for a sustainable energy system [1]. World consumption of hydrogen is expected to increase 3.5 percent annually to more than 300 billion cubic meters, not only for conventional industrial uses, such as petroleum refinery, chemical production, food processing, pharmaceutical or metal processing, but also for clean energy technologies, such as fuel cell vehicles and bio-refinery. Global hydrogen production mostly comes from natural gas (48%), oil (30%) and coal (18%), water electrolysis accounting for only 4% [2]. The most established technology to produce hydrogen on a commercial scale is nowadays the steam methane reforming (SMR) of natural gas. The synthesis gas is the typical intermediate for hydrogen production. High temperature- and low temperature water-gas shift (WGS) reactions are extensively used to increase the hydrogen content in the synthesis gas. Commercially, the syngas is usually passed through a dual-stage WGS reaction, with two reactors in series: a high temperature reactor (300-450 °C) and a low temperature reactor (180-270 °C). The high temperature reactor usually contains an iron oxide catalyst to convert bulk CO from ~15% to ~3%, whereas the low temperature reactor normally contains a copper catalyst for reducing the CO level to less than 0.4% [3, 4]. In the WGS reactors, CO reacts with water and produces CO_2 and H_2 by Eq. 1:

$$CO + H_2O \leftrightarrow CO_2 + H_2 \quad (1)$$

The product gas coming out from the low temperature WGS reactor still contains a high amount of CO, which is not suitable for certain uses, such as low temperature fuel cells [5]. It is well known that the fuel cell technology offers a highly efficient conversion of chemical energy into electrical energy without emission of environmental pollutants, thereby making fuel cells one of the most promising sources of power generation [5, 6]. Proton exchange membrane (PEM) fuel cells are a promising type of low temperature fuel cell being developed for transport applications as well as for stationary and portable fuel cell applications. The major challenge for low temperature fuel cell is that they are extremely sensitive towards impurities such as CO_x. The CO concentration in the hydrogen gas stream is typically required to be lower than 10 ppm [7]. Purification of the hydrogen stream is then essential, and several technologies are under development to produce fuel cell grade hydrogen, such as preferential oxidation (PROX) [5, 8, 9], selective methanation [10-12], sorption enhanced water gas shift (SEWGS) reaction [13-16] and pressure swing adsorption (PSA) [17, 18]. In some cases, following the shift reactors, the syngas is fed to a CO_2 capture unit based on physical solvents like selexol, rectisol, or chemical ones like amine-based solvents. However, for a high purity hydrogen production, a PSA unit is needed as final step.

Therefore, it is deduced that the removal of CO_x up to obtain ppm levels in a hydrogen stream makes the overall process quite complex, lengthy and with low yield, which hinders the application of the existing technology for hydrogen production in vehicular and small-scale fuel cell applications. Furthermore, besides the consumption of fossil fuels, the overall process entails high capital costs [19]. Thus,

[a]SINTEF Industry, Norway
[b]Department of Chemical Engineering, Norwegian University of Science and Technology, Sem Sælands vei 4, Trondheim, NO-7491, Norway
E-mail: kumarranjan.rout@sintef.no
E-mail: de.chen@ntnu.no

the development of more energy-efficient and cost-effective technologies for pure hydrogen production is highly desired. Hence, it is essential to find new routes for the removal of CO from hydrogen streams with the specific objective of application in fuel cell systems, which are highly selective and low-cost processes that provide the high yields of hydrogen needed. In the present work, the sorption enhanced Boudouard (SEB) reaction is purposed as a one-step high-purity hydrogen production process, which could greatly simplify the procedure, increase the energy efficiency and reduce costs.

Nowadays, an important research work is being carried out on the calcium looping process (CaL), which is a calcium sorbent-based chemical looping process that has the potential to increase the H_2/CO ratio [20]. The CaL integrates the WGS reaction with in-situ CO_2, sulfur and halide removal at high temperatures in a single-stage reactor. It utilizes a high temperature regenerable calcium oxide-based sorbent (CaO), which apart from capturing the CO_2, enhances the yield of H_2 and simultaneously captures sulfur and halide impurities. However, it introduces issues and costs associated with the separation of the sorbent and catalyst prior to calcination, with the pretreatment of the catalyst to the active form after its deactivation in the presence of CO_2 in the calciner at high temperatures, as well as with the replacement of the spent catalyst [21]. Recently, the WGS reaction has been performed in the presence of only a CaO sorbent [21]. The results obtained lead to the conclusion of that the WGS reaction takes place to a considerable extent even in the absence of a metal catalyst at relatively higher temperatures than the conventional WGS process. Thus, high purity H_2 can be produced with very low levels of CO and CO_2 during the pre-breakthrough region of the sorption curve while the CaO sorbent is active. However, the yield of H_2 has not been reported in that study [21]. It is believed that the high purity of H_2 is due to the shifting of the reaction equilibrium to the forward direction when the CO_2 formed is removed by the CaO. However, the possible interaction between CO and CaO has not been studied properly yet. Therefore, in the present work an attempt has been made for the first time to study the feasibility of the reaction between CO and CaO via the Sorption Enhanced Boudouard (SEB) reaction to increase the ratio of H_2/CO in the syngas.

In this work, we illustrate the feasibility of highly selective removal of CO by the SEB reaction up to reach ppm levels without consumption of hydrogen by thermodynamic analysis and experimental demonstration. We further demonstrate the feasibility of a continuous process by a cyclic carbonate looping process where the carbon formed by the SEB reaction can be burned effectively in air to supply heat for the regeneration of the saturated CaO materials. We study the effects of operation conditions, such as the concentration of H_2 and the temperature, on the activity of the SEB reaction. We also demonstrate a remarkable reduction of the CO concentration from 0.5% in a syngas up to 5-10 ppm, which is suitable for low temperature fuel cells and avoids a subsequent preferential oxidation process. An oxygen vacancy mediated catalytic cycle of Boudouard reaction on calcium oxide is proposed in this study.

2. Experimental

2.1. CO_2 sorbent

Arctic dolomite was supplied by Franefoss Miljøkalk As, Norway. This has a purity of approximately 98.5 wt.% $CaMg(CO_3)_2$ and no sulfur according to X-ray fluorescence analysis. The dolomite was used as a precursor of CaO for the capture of CO_2. The initial maximum CO_2 capture capacity was estimated as being 0.46 g CO_2/g sorbent. The dolomite was ground and sieved to reach a particle size of 250-500 µm. It was calcined in an air flow (200 mL min^{-1}) at 900 °C for 4 h prior to its storage.

2.2. Experimental procedure

The SEB reaction experiments were carried out by passing the gas mixture over dolomite in a homemade fixed bed reactor thermogravimetric analyzer (TGA), where a good gas-solid contact is obtained. Gases were delivered by Bronkhorst® mass flow controllers. The dolomite, 3-20 gm sample, was inserted in the stainless tube fixed bed reactor, while the reactor is suspended from an electronic balance. A mass spectrometer (MS) was used to analyze the gas evolved during the experiments. The experiments were performed at 420-550 °C and 1 atm. A cyclic experiment was also carried out using a regeneration step at 800 °C in an N_2 or air flow (1 NL min^{-1}). The regeneration temperature was selected taking into consideration the thermodynamic limitations of the decarbonation reaction and the kinetics of the decarbonation of dolomite [22].

The dolomite sample was exposed to the inlet gas mixture for a time sufficiently long (approximately 250 minutes) to determine the weight gain of the sorbent. Thus, the weight change of the dolomite sample was continuously monitored.

3. Thermodynamic analysis of sorption enhanced Boudouard reaction on CaO

The Boudouard reaction is the redox reaction to form carbon dioxide and solid carbon from carbon monoxide, as it is shown in Eq. 2 [23]:

$$2CO \leftrightarrow CO_2 + C \qquad \Delta H = -172 \text{ kJ/mol} \qquad (2)$$

The Boudouard reaction is reversible and exothermic at all temperatures. However, at high temperatures (typically>700 ºC), when the large positive entropic term ($T{\cdot}\Delta S$) prevails the enthalpic component, the Gibbs free energy becomes negative ($\Delta G{=}\Delta H{-}T{\cdot}\Delta S$) and the reaction proceeds spontaneously to produce CO [24]. Likewise, at lower temperatures the forward exothermic reaction toward the formation of CO_2 is favored, but the conversion is limited by thermodynamics. Based on Le Chatelier's principle, the removal of CO_2 in-situ by carbonation of an alkaline metal oxide such as CaO (Eq. 3) could enhance the conversion. The total reaction (Eq. 4) is called sorption enhanced Boudouard reaction, which is highly exothermic.

$$CaO + CO_2 \leftrightarrow CaCO_3 \qquad \Delta H = -178 \text{ kJ/mol} \qquad (3)$$

The overall SEB reaction is shown in Eq. 4 as follows:

$$CaO + 2CO \leftrightarrow CaCO_3 + C \qquad \Delta H = -350 \text{ kJ/mol} \qquad (4)$$

Thermodynamic analyses of the Boudouard and the SEB reactions were conducted between 400 and 700 °C. The equilibrium composition was estimated by minimization of the Gibbs free energy of the system using Aspen Plus 8.6 software. The RGibbs reactor was specified as the reaction system and the Peng-Robinson thermodynamic package as the property method. The species included in the product pool were CO, CO_2, C (graphite as solid carbon), CaO and $CaCO_3$. The equilibrium partial pressure of CO as a function of temperature in a range of 400 and 700 °C is plotted in Fig. 1 for the thermodynamic analysis of both the SEB reaction and the Boudouard reaction. The results illustrate that the equilibrium partial pressure of CO for the SEB reaction is much lower than that for the Boudouard reaction at all the temperatures studied, clearly indicating the sorption enhanced effects. Moreover, for the SEB reaction at 400 °C, the CO and CO_2 partial pressure values are close to zero, while between 400 and 450 °C only CO is present. This means that in the 400-450 °C temperature range almost all the CO_2 formed is captured by the sorbent. It suggested that fuel cell grade hydrogen (CO content less than 10 ppm) can be obtained by fixation of CO to solids through the SEB reaction at mediate temperatures. In addition, based on Le Chatelier's principle high pressure shifts the reaction towards $CaCO_3$ and C formation, thus enhancing the conversion of CaO.

The equilibrium CO_2 concentration for the SEB reaction increases concurrently with increasing temperature because of the unfavorable thermodynamics of the carbonation reaction at high temperature. This led to a weaker sorption enhancement at higher temperatures, which is reflected by the increase in the CO concentration as temperature increases.

The sorbent can be regenerated by air or oxygen following the Eq. (5):

$$CaCO_3 + C + O_2 \leftrightarrow CaO + 2CO_2 \quad \Delta H = -41 \text{ kJ/mol} \quad (5)$$

The highly exothermic oxidation of solid carbon is effectively coupled with the highly endothermic decarbonation reaction. The regeneration is weakly exothermic. The overall cycle of SEB and regeneration is also an exothermic reaction. The temperature required for the regeneration depends on the equilibrium of the decarbonation of $CaCO_3$.

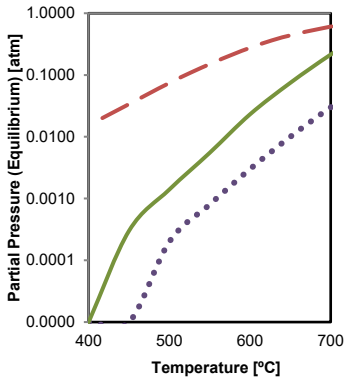

Fig. 1. Equilibrium partial pressure of CO (— —) vs. temperature for the Boudouard reaction, and equilibrium partial pressures of CO (—) and CO_2 (•••) vs. temperature for the sorption enhanced Boudouard (SEB) reaction.

Using air for regeneration not only has the advantage of low cost, since it avoids expensive air purification for pure oxygen production, but also it lowers the temperature required for regeneration by decreasing the CO_2 pressure.

A relevant advantage of using the SEB reaction for the removal of CO is that it does not require a metal catalyst or steam during the reaction. The decomposition of CO by the Boudouard reaction to form carbon is a very slow reaction and hence is usually catalyzed by transition metals such as Fe, Ni or Co [25]. A CO_2 sorbent has previously been used in literature [26, 27] to enhance the purity of hydrogen from syngas using the Boudouard reaction in conjunction of water gas shift reaction, but using metal catalysts and steam. However, it will be demonstrated in the present work that the SEB reaction would avoid the need of using a conventional catalyst by the shifting of the reaction equilibrium through the in situ CO_2 removal by a CO_2 sorbent. An additional advantage of the SEB reaction is that the thermodynamic analysis (one mole of CO_2 is formed from two moles of CO) indicates that it is favored at higher pressures, so the efficiency of the CO disproportionation via the Boudouard reaction will be expected to increase at elevated pressures.

4. Results and discussion

4.1. Sorption enhanced Boudouard (SEB) reaction

For the SEB reaction, thermodynamic analysis in Fig. 1 indicates that at 450 °C the CO level is 3 ppm and the CO_2 level is 0.1 ppm. The CO level increases from 3 ppm at 450 °C to 10 ppm at 490 °C. This implies that the SEB reaction can produce such low CO and CO_2 levels as required for low temperature fuel cells. Fig. 2 shows the experimental results of the SEB reaction in a CO_2/CO/H_2/N_2 gas mixture on dolomite at 550 °C during the carbonation stage. The concentrations of CO_2, CO and H_2 in the gas mixture simulated the syngas composition. Afterwards, decarbonation was carried out in N_2 at 800 °C. The weight change, Δw, of the dolomite as a function of the time of experiment (TOS: time on stream) is shown in Fig. 2a, while the outlet gas concentrations during the carbonation stage as a function of the TOS are shown in Fig. 2b. The gas consumption rates of CO and CO_2 are shown as a function of TOS in Fig. 2c.

Fig. 2b shows that the outlet CO_2 concentration increases rapidly reaching the value of the inlet concentration (15 vol.%). Afterwards, the outlet CO_2 concentration becomes slightly higher than the inlet CO_2 concentration, indicating that additional CO_2 is formed via the Boudouard reaction. The outlet concentration of CO is much lower than the inlet CO concentration and gradually decreases with TOS. Fig. 2c shows the gas consumption rates of CO and CO_2 with the time, where the initial CO_2 consumption rate is very high, but it experiences a very fast decrease and is almost zero after approximately 36 minutes of TOS. The weight of the dolomite increases concurrently with TOS (Fig. 2a) even after 36 minutes. The weight decreases after about 100 min, which is a result of the decarbonation of the sorbent in N_2 at 800 °C, as shown in Fig. 2a. It is interesting to note that a mass of 0.17 g/g dolomite was remained after the complete decarbonation (Fig. 2a). On an assumption of full carbonation of CaO with the CO_2 generated by the Boudouard reaction, the weight ratio of CO_2 and C is 3.66. The ratio between the weight loss of CO_2 release and the weight remained is 2.83, which is

lower than the theoretic value of 3.66 for the Boudouard reaction. It suggests that only part of the CO_2 generated by the Boudouard reaction is captured by the carbonation reaction. The remained material was confirmed to be carbon by oxidation in air (Fig. 3), SEM (Fig. 5a) and Raman spectroscopy analysis (Fig. 5b). This agrees with the observation of Mondal et al. [28] in experiments on the separation of hydrogen from syngas using solid oxides, where significant carbon deposition due to the Boudouard reaction resulted in the deactivation of the oxides surfaces as a result of an insulated layer of carbon. All the results reveal that sorption enhanced Boudouard (SEB) takes place, where CO dissociates by the Boudouard reaction and it is converted to CO_2 and solid carbon, while CO_2 formed is captured by the CaO in the dolomite, in turn enhancing the Boudouard reaction.

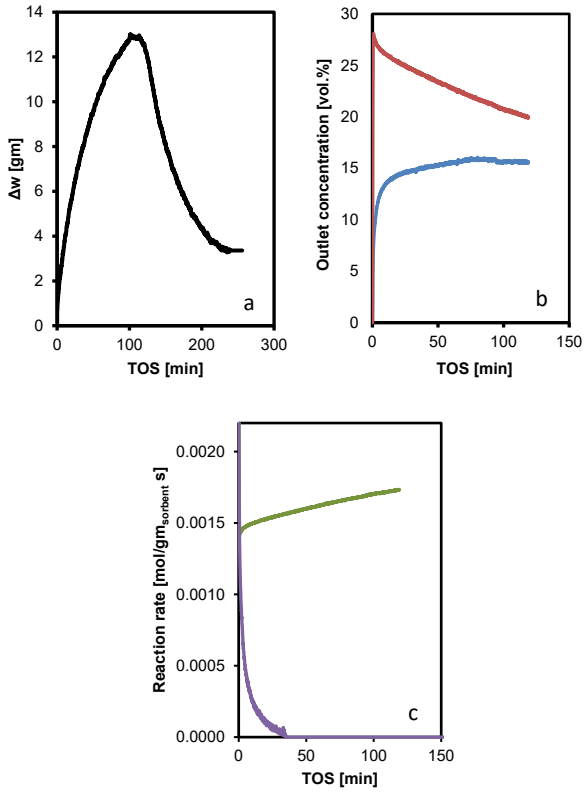

Fig. 2. Weight change, Δw, of the dolomite sorbent (—) (a), outlet CO (—) and CO_2 (—) concentrations (b), and reaction rate of CO (—) and CO_2 (—) (c) vs. time on stream (TOS) during an experiment with P_{CO2}=0.15 bar + P_{CO}=0.65 bar + P_{H2}=0.12 bar (balance N_2). Experimental conditions: $T_{carbonation}$=550 °C, $T_{calcination}$=800 °C (P_{N2}=1 bar), dolomite=20 gm.

The results might suggest competitive reactions on CaO surface between the direct carbonation of CO_2 and the Boudouard reaction followed by the carbonation reaction. The surface Boudouard reaction possibly suppresses the direct carbonation of the CO_2 in the gas phase. To confirm this hypothesis, Fig. 3 shows a comparison of the weight gains during experiments with CO_2/N_2 and $CO_2/CO/N_2$ gas mixtures using identical CO and CO_2 pressures as in the previous experiment. The initial increase in the weight followed almost an identical rate for both mixtures. Taking into account the results in Fig. 2b, showing a fast increase in the CO_2 concentration, it can be suggested that direct CO_2 carbonation takes place initially. Thus, the rate of weight increase was slower for the CO/CO_2 mixture than in the experiment with only CO_2. A more significant difference was observed in the regeneration step in N_2. The $CaCO_3$ formed in the experiment with only CO_2 was completely regenerated, which was indicated by the complete weight loss, while the weight gained in the experiment with the CO/CO_2 mixture was only partially lost, and the ratio of maximum weight and the remained weight was about 2.09, again lower than the theoretic value of 3.66. These results suggest that the SEB reaction is more preferable than the direct CO_2 carbonation, although the reaction rate of SEB is lower than that of direct carbonation.

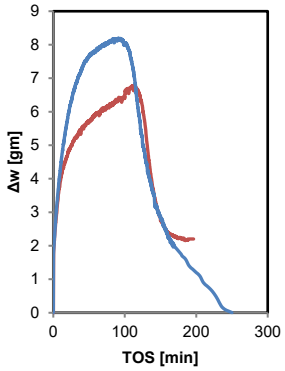

Fig. 3. Weight change, Δw, of the dolomite sorbent vs. time on stream (TOS) during experiments with P_{CO2}=0.15 bar (—) and with P_{CO2}=0.15 bar + P_{CO}=0.65 bar (—) (balance N_2). Experimental conditions: $T_{carbonation}$=550 ºC, $T_{calcination}$=800 ºC (P_{N2}=1 bar), dolomite=20 gm.

By comparing Fig. 2a and Fig. 3, it can be deduced that the presence of H_2 in the gas mixture significantly enhanced the SEB reaction. The average formation rate of carbon within 100 minutes increased from 1.1 to 1.7 mg/$g_{dolomite}$,min and the weight ratio of CO_2 captured to C formed increased from 2.09 to 2.83, when hydrogen is added. It means that the average SEB rate increased from 0.091 to 0.14 mmol/$g_{dolomite}$,min.

Carbon formed by the SEB reaction was studied by SEM analysis (Fig. 4a). After the SEB reaction, the solid material (sorbent and carbon) was washed to remove $CaCO_3$ and unconverted CaO, while carbon was collected and analyzed by SEM. It can be seen that the carbon formed by the SEB reaction shows very thin crystalline sheets. Fig. 5a also shows that several graphene layers stacked with each other. Fig. 5b shows the Raman spectra of the carbon produced from the SEB reaction. The obtained Raman spectra is identical to that reported in the literature for graphite material [29]. The G and D peaks of Raman spectra lie around 1560 cm^{-1} and 1360 cm^{-1}, respectively. This indicates that the carbon formed by the SEB reaction is highly graphitic.

These results clearly demonstrated that the SEB reaction takes place in the absence of a conventional metal catalyst. It is therefore suggested that CaO present in the dolomite produces a catalytic effect over the Boudouard reaction under the studied conditions. Previous studies in the literature have reported that calcined dolomite can act as both CO_2 sorbent and catalyst on sorption enhanced water gas shift experiments and that no addition of

conventionally employed catalysts (metals, metal oxides) is required [30, 31]. In the present work, CaO in calcined dolomite could therefore be responsible for the activity towards the Boudouard reaction, which would mean that calcined dolomite (CaO) may act as both catalyst and CO_2 sorbent in the SEB process. It could be argued that Fe and other metals in dolomites can serve as catalysts for the Boudouard reaction. In order to check the possible effect of the metal impurities contained in dolomites on the SEB, a reference run was performed on a synthetic CaO material with a purity of 99.99% using a gas mixture of CO and H_2 at 550 °C, as shown in Fig. 5. It shows that weight is gained with an almost constant rate of 7.1 $mg/g_{dolomite}$,min. This confirms that the CaO present in the dolomite can effectively be responsible for the activity towards the SEB reaction.

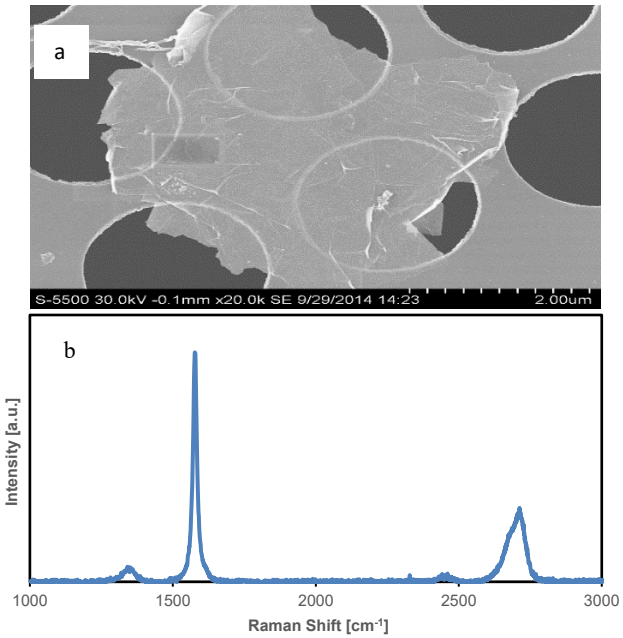

Fig. 4. Structural characterization of the carbon produced by the SEB reaction: SEM image (a) and Raman spectra (b).

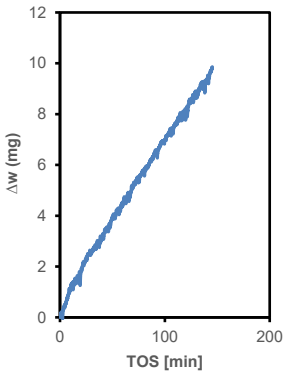

Fig. 5. Weight change, Δw, of the CaO-based synthetic sorbent vs. time on stream (TOS) during an experiment with P_{CO}=0.25 bar + P_{H2}=0.75 bar. Experimental conditions: $T_{carbonation}$=550 °C, synthetic sorbent=10 gm.

4.2. Selective removal of CO for pure hydrogen production

Selective removal of CO from the CO/H_2 mixture (0.5/99.5 molar ratio) was carried out on dolomite in the TGA-fixed bed reactor at 420 °C. Fig. 6a shows the weight change of the dolomite, while Fig. 6b shows the outlet CO concentration as a function of the time on stream. A very low CO concentration (<5 ppm) was detected during all the experimental time of about 12 hours. The weight of the dolomite increased concurrently with time on stream. The detected increase in the weight accounts well for the captured CO_2 and the deposited carbon generated by the SEB reaction based on the mass balance. The results clearly demonstrate the SEB reaction as a new effective route to produce fuel-cell grade H_2 without loss of hydrogen.

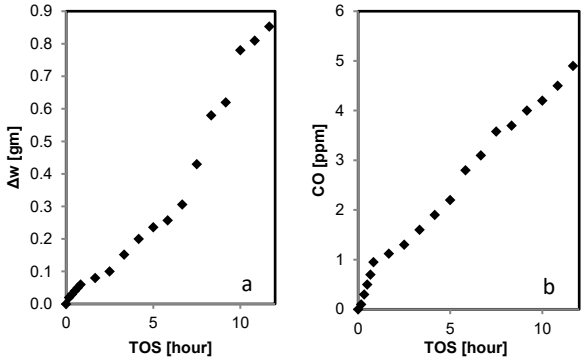

Fig. 6. Weight change, Δw, of the dolomite sorbent (a) and outlet CO concentration (b) vs. time on stream (TOS) during an experiment with P_{CO}=0.005 bar + P_{H2}=0.995 bar. Experimental conditions: $T_{carbonation}$=420 °C, dolomite=3 gm.

The effect of the temperature on the SEB reaction in a CO/H_2 gas mixture is shown in Fig. 7. The weight change of the dolomite at 450 and 550 °C as a function of the time of experiment is shown in Fig. 7a, whereas the outlet gas concentrations for the experiment at 550 °C as a function of the time of experiment are shown in Fig. 7b.

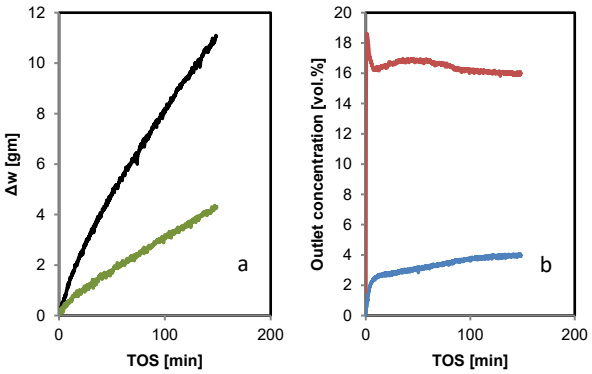

Fig. 7. (a) Weight change, Δw, of the dolomite sorbent during carbonation experiments at 450 °C (—) and 550 °C (—) with P_{CO}=0.25 bar + P_{H2}=0.75 bar; (b) Outlet CO (—) and CO_2 (—) concentrations vs. time on stream (TOS) during the carbonation experiment at 550 °C with P_{CO}=0.25 bar + P_{H2}=0.75 bar. Experimental conditions: dolomite=10 gm.

The dolomite experiences a much higher increase in its weight when the experiment is performed at 550 °C (Fig. 7a), which means that a higher amount of CO_2 is captured by the sorbent and a higher deposition of carbon is taking place, i.e. the reaction rate of the SEB reaction increases with the increasing in temperature. Despite the favorable thermodynamics of the carbonation reaction at low temperature, which favors the SEB reaction, the kinetics of the process at low temperature is slower. Fig. 7b shows that the outlet CO_2 concentration increases during the time of experiment as the sorbent is being saturated and loses capacity for the removal of CO_2. The increase in the CO_2 concentration is the result of its formation via the SEB reaction. Likewise, the outlet CO concentration increases with time (Fig. 7b) and it is lower than the inlet CO concentration along the experiment.

Cyclic experiments were carried out with a CO/H_2 gas mixture on dolomite at 550 °C during the carbonation stage and at 800 °C in N_2 during the regeneration step, which is followed by a combustion step in air in order to eliminate the deposited carbon. The cycle stability of the CO_2 sorbent for the SEB reaction was tested in four carbonation/decarbonation cycles. Fig. 8 shows the weight change of the dolomite as a function of the time along the cycles. The results remain quite constant during the four cycles, which indicates no significant decrease in the CO_2 capture capacity of the sorbent. Captured CO_2 was calculated to be 4.6 gm/10 g dolomite in average of all the cycles. The weight ratio of CO_2 to C is almost constant with a value of about 0.75 in all the cycles, which is much lower than the stoichiometric value of 3.66 for the Boudouard reaction.

After the calcination step, the remaining weight change is 6.8 gm in average, which means 0.68 $g_{carbon}/g_{fresh\ sorbent}$. This amount of carbon is higher than that shown in Fig. 2a, but in the cyclic experiment no CO_2 had been added in the gas mixture and the concentration of H_2 is quite higher.

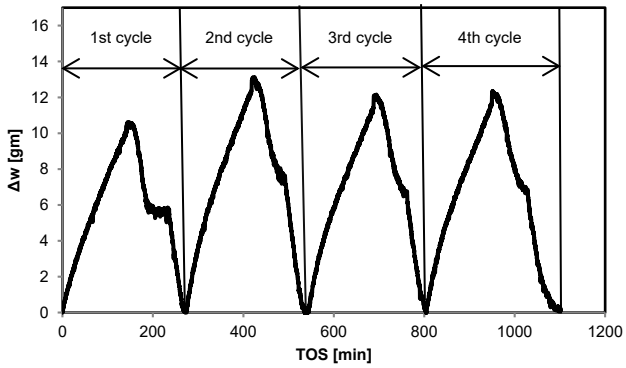

Fig. 8. Weight change, Δw, of the dolomite sorbent vs. time on stream (TOS) for several cycles during an experiment with P_{CO}=0.25 bar + P_{H2}=0.75 bar. Experimental conditions: $T_{carbonation}$=550 °C, $T_{calcination}$=800 °C (P_{N2}=1 bar or P_{air}=1 bar), dolomite=10 gm.

4.3. On the reaction mechanism

Surface science and density functional theory (DFT) calculation on CO and CO_2 interaction with CaO have been reported in the literature and they provide mechanistic insights [32]. CO_2 and CO interaction with CaO surfaces has been studied by surface science techniques such as Metastable Induced Electron Spectroscopy (MIES), Ultraviolet Photoelectron Spectroscopy (UPS) and X-ray Photoelectron Spectroscopy (XPS) on CaO films [32]. Since CaO has not density of states near the Fermi level, no CO_2 and CO dissociation is possible. The CO_2 molecules impinge on the surface and form CO_3^{2-} complexes with surface oxygen atoms. According to Kadossov et al. [33], the interaction between CO molecules and CaO(100) single crystal surfaces is very weak. Non-dissociative CO adsorption is found only at irregular sites, e.g. edges [33]. However, the formation of CO_3^{2-} complexes was clearly observed by MIES and XPS when the CaO surface was exposed to CO, although the mechanism for the formation of CO_3^{2-} complexes is unclear. DFT calculations [34, 35] predicted that these CO molecules are adsorbed via their C atoms on Ca sites, but rather weakly. On the polycrystalline CaO surfaces, no significant contributions from molecularly adsorbed CO were found in MIES or UPS spectra [32]. However, a UV-Visible and IR spectroscopic study of the adsorption of CO on microcrystalline MgO and CaO showed two types of adsorbed species, such as lower order non-reduced species incorporating surface oxide ions with $Ca^{2+}\ldots(CO_2)^{2-}$ stoichiometry, and reduced polymeric species like cyclic anion species $(CO)_n^{2-}$ [36]. The formation of $(CO_3)^{2-}$ was then proposed like:

$$CO + O^{2-} = (CO_2)^{2-} + V_O \quad (6)$$

$$(CO_2)^{2-} + nCO = (C_{n+1}O_{n+2})^{2-} \quad (7)$$

$$(C_{n+1}O_{n+2})^{2-} + O^{2-} = (C_nO_n)^{2-} + (CO_3)^{2-} + V_O \quad (8)$$

where V_O is the oxygen vacancy. The proposed mechanism involved the formation of surface species $(CO_2)^{2-}$ and the formation of reduced polymeric species such as $(C_{n+1}O_{n+2})^{2-}$. By the intervention of a further surface oxygen ion, ring closure occurs to give a resonance-stabilized polymeric carbanion $(C_nO_n)^{2-}$ and a carbonate species is rejected in the surface. This happened predominantly at n=5 on CaO [36]. Atomic-scale simulation, by means of density functional calculations and molecular dynamic simulation, has also been applied to understand the mechanism of carbonation of CaO. It pointed out O and C vacancies as thermally important defects, together with interstitial O. The joint C and O diffusion via vacancy mechanisms is important for CO_2 diffusion within $CaCO_3$ and $CaCO_3$ growth. Formation and diffusion of $(CO_3)^{2-}$ in the lattice of CaO generates the surface oxygen vacancy. The in-situ generated O vacancy seems to facilitate the CO dissociation, CO → C + O, and then O fills the surface oxygen vacancy, that reacts further with an undissociated $CO_{(ads)}$ to form surface $CO_{2(ads)}$ [37, 38]. Based on above discussion, a reaction mechanism of SEB is proposed in the scheme in Fig. 9:

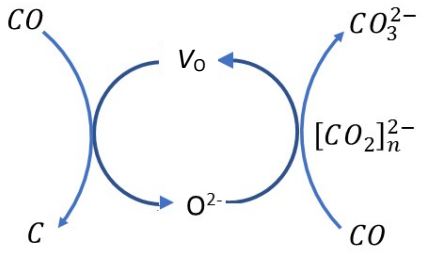

Fig. 9. The proposed reaction mechanism of the SEB reaction.

The main feature of the mechanism is the oxygen vacancy as the active site for the SEB reaction, which is generated in-situ by CO

adsorption (Fig. 9). Moreover, the results in the present work have clearly revealed that hydrogen enhanced the SEB reaction. It could possibly suggest the hydrogen assisted CO activation on the oxygen vacancy, although the detailed mechanism needs to be further studied.

5. Conclusions

The proposed SEB process integrates the Boudouard reaction with in situ CO_2 removal in a single step on a CaO based material, which not only catalyzes the Boudouard reaction but also removes the generated CO_2 in situ. The direct tandem reaction on CaO by the formation of $CaCO_3$ shifts the Boudouard reaction to a forward direction following the Le Chatelier's principle, thus enhancing the CO conversion. Here we demonstrated the feasibility of the removal of CO without consumption of hydrogen by the SEB reaction on dolomite in the absence of conventional noble metal catalysts, achieving a CO concentration lower than 5 ppm. The presence of hydrogen enhanced the SEB reaction. This new process can replace the hydrogen purification processes such as methanation, which consumes hydrogen, or selective oxidation of CO, which requires pure oxygen and also consumes a part of the hydrogen. In addition, the SEB reaction combines the purification process with the CO_2 removal process, such as pressure swing process, in one-step. Moreover, the process allows the production of pure hydrogen with ultra-low concentrations of CO and CO_2. The low temperature PEM fuel cell can benefit from such ultra-pure hydrogen. An oxygen vacancy mediated catalytic cycle of Boudouard reaction on metal oxide is proposed, including CO dissociation and CO reaction with lattice oxygen. It is expected that the chemistry of CO reaction on CaO can be also applied to other metal oxides as well as to process beyond CO removal, such as CO hydrogenation on metal oxides.

Acknowledgements

This work was carried out with financial support from the iCSI center for Research-based Innovation.

Notes and references

[1] B. Balasubramanian, A. Lopez Ortiz, S. Kaytakoglu, D.P. Harrison, Hydrogen from methane in a single-step process, Chemical Engineering Science, 54 (1999) 3543-3552.
[2] R.B. Gupta, Hydrogen fuel : production, transport, and storage Boca Raton, FL : CRC Press (2009).
[3] P. Häussinger, R. Lohmüller, A.M. Watson, Hydrogen, Ullmann's Encyclopedia of Industrial Chemistry, (2000).
[4] A.F. Ghenciu, Review of fuel processing catalysts for hydrogen production in PEM fuel cell systems, Current Opinion in Solid State and Materials Science, 6 (2002) 389-399.
[5] T. Choudhary, Goodman, DW., CO-free fuel processing for fuel cell applications, Catalysis Today, 77 (2002) 65-78.
[6] A. Appleby, Foulkes, FR., Fuel Cell Handbook, Van Nostrand Reinhold, New York,, (1989).
[7] N.A. Koryabkina, A.A. Phatak, W.F. Ruettinger, R.J. Farrauto, F.H. Ribeiro, Determination of kinetic parameters for the water–gas shift reaction on copper catalysts under realistic conditions for fuel cell applications, Journal of Catalysis, 217 (2003) 233-239.
[8] J. Saavedra, T. Whittaker, Z. Chen, C.J. Pursell, R.M. Rioux, B.D. Chandler, Controlling activity and selectivity using water in the Au-catalysed preferential oxidation of CO in H2, Nat Chem, 8 (2016) 584-589.
[9] E. Newson, T.B. Truong, N. De Silva, A. Fleury, R. Ijpelaar, 85 High selectivity preferential oxidation (PROX) catalysts for CO removal from hydrocarbon derived reformates for PEM fuel cells, in: M.O. Masakazu Anpo, Y. Hiromi (Eds.) Studies in Surface Science and Catalysis, Elsevier, 2003, pp. 391-394.
[10] C. Galletti, S. Specchia, V. Specchia, CO selective methanation in H2-rich gas for fuel cell application: Microchannel reactor performance with Ru-based catalysts, Chemical Engineering Journal, 167 (2011) 616-621.
[11] H. Yoshida, K. Watanabe, N. Iwasa, S.-i. Fujita, M. Arai, Selective methanation of CO in H2-rich gas stream by synthetic nickel-containing smectite based catalysts, Applied Catalysis B: Environmental, 162 (2015) 93-97.
[12] K. Hayashi, T. Miyao, Y. Tabira, K. Higashiyama, Low-temperature Selective CO Methanation over Unsupported Nickel Catalyst Covered by Silica Thin Layer, Journal of the Japan Petroleum Institute, 59 (2016) 65-71.
[13] T. Noor, M.V. Gil, D. Chen, Production of fuel-cell grade hydrogen by sorption enhanced water gas shift reaction using Pd/Ni–Co catalysts, Applied Catalysis B: Environmental, 150–151 (2014) 585-595.
[14] C.R. Müller, R. Pacciani, C.D. Bohn, S.A. Scott, J.S. Dennis, Investigation of the Enhanced Water Gas Shift Reaction Using Natural and Synthetic Sorbents for the Capture of CO2, Industrial and Engineering Chemistry Research, 48 (2009) 10284-10291.
[15] L. He, D. Chen, Single-Stage Production of Highly Concentrated Hydrogen from Biomass-Derived Syngas, ChemSusChem, 3 (2010) 1169-1171.
[16] R.W. Stevens Jr, A. Shamsi, S. Carpenter, R. Siriwardane, Sorption-enhanced water gas shift reaction by sodium-promoted calcium oxides, Fuel, 89 (2010) 1280-1286.
[17] B. Li, G. He, X. Jiang, Y. Dai, X. Ruan, Pressure swing adsorption/membrane hybrid processes for hydrogen purification with a high recovery, Frontiers of Chemical Science and Engineering, 10 (2016) 255-264.
[18] E.H. Majlan, W.R. Wan Daud, S.E. Iyuke, A.B. Mohamad, A.A.H. Kadhum, A.W. Mohammad, M.S. Takriff, N. Bahaman, Hydrogen purification using compact pressure swing adsorption system for fuel cell, International Journal of Hydrogen Energy, 34 (2009) 2771-2777.
[19] B. Dou, C. Wang, H. Chen, Y. Song, B. Xie, Continuous sorption-enhanced steam reforming of glycerol to high-purity hydrogen production, International Journal of Hydrogen Energy, 38 (2013) 11902-11909.
[20] L. Fan, F. Li, S. Ramkumar, Utilization of chemical looping strategy in coal gasification processes, Particuology, 6 (2008) 131-142.
[21] S. Ramkumar, L.-S. Fan, Calcium Looping Process (CLP) for Enhanced Noncatalytic Hydrogen Production with Integrated Carbon Dioxide Capture, Energy & Fuels, 24 (2010) 4408-4418.
[22] L. He, H. Berntsen, D. Chen, Approaching Sustainable H_2 Production: Sorption Enhanced Steam Reforming of Ethanol, Journal of Physical Chemistry A, 114 (2010) 3834-3844.
[23] O. Boudouard, C.R. Acad. Sci, Paris 128, 824 and 1521, (1899).
[24] P. Lahijani, Z.A. Zainal, M. Mohammadi, A.R. Mohamed, Conversion of the greenhouse gas CO2 to the fuel gas CO via the Boudouard reaction: A review, Renewable and Sustainable Energy Reviews, 41 (2015) 615-632.

[25] E.T. Turkdogan, J.V. Vinters, Catalytic effect of iron on decomposition of carbon monoxide: I. carbon deposition in H2-CO Mixtures, MT, 5 (1974) 11-19.
[26] T. Wiltowski, K. Mondal, A. Campen, D. Dasgupta, A. Konieczny, Reaction swing approach for hydrogen production from carbonaceous fuels, International Journal of Hydrogen Energy, 33 (2008) 293-302.
[27] A. Campen, K. Mondal, T. Wiltowski, Separation of hydrogen from syngas using a regenerative system, International Journal of Hydrogen Energy, 33 (2008) 332-339.
[28] K. Mondal, K. Piotrowski, D. Dasgupta, E. Hippo, T. Wiltowski, Hydrogen from Coal in a Single Step, Industrial & Engineering Chemistry Research, 44 (2005) 5508-5517.
[29] A.C. Ferrari, Raman spectroscopy of graphene and graphite: Disorder, electron–phonon coupling, doping and nonadiabatic effects, Solid State Communications, 143 (2007) 47-57.
[30] M.A. Escobedo Bretado, M.D. Delgado Vigil, J.S. Gutiérrez, A. López Ortiz, V. Collins-Martínez, Hydrogen production by absorption enhanced water gas shift (AEWGS), International Journal of Hydrogen Energy, 35 (2010) 12083-12090.
[31] C. Han, D.P. Harrison, Simultaneous shift reaction and carbon dioxide separation for the direct production of hydrogen, Chemical Engineering Science, 49 (1994) 5875-5883.
[32] F. Voigts, F. Bebensee, S. Dahle, K. Volgmann, W. Maus-Friedrichs, The adsorption of CO2 and CO on Ca and CaO films studied with MIES, UPS and XPS, Surface Science, 603 (2009) 40-49.
[33] E. Kadossov, U. Burghaus, Adsorption kinetics and dynamics of CO, NO, and CO2 on reduced CaO(100), Journal of Physical Chemistry C, 112 (2008) 7390-7400.
[34] W.S.A. Halim, CO adsorption on MgO, CaO and SrO crystals periodic Hartree-Fock calculations, Applied Surface Science, 253 (2007) 8974-8980.
[35] M. Bajdich, J.K. Norskov, A. Vojvodic, Surface energetics of alkaline-earth metal oxides: Trends in stability and adsorption of small molecules, Physical Review B, 91 (2015).
[36] E. Garrone, A. Zecchina, F.S. Stone, CO ADSORPTION ON MGO AND CAO - SPECTROSCOPIC INVESTIGATIONS OF STAGES PRIOR TO CYCLIC ANION CLUSTER FORMATION, Journal of the Chemical Society-Faraday Transactions I, 84 (1988) 2843-2854.
[37] A.K. Kandalam, B. Chatterjee, S.N. Khanna, B.K. Rao, P. Jena, B.V. Reddy, Oxidation of CO on Fe2O3 model surfaces, Surface Science, 601 (2007) 4873-4880.
[38] G. Lanzani, A.G. Nasibulin, K. Laasonen, E.I. Kauppinen, CO dissociation and CO+O reactions on a nanosized iron cluster, Nano Research, 2 (2009) 660-670.

